Nonlinear Dyn (2015) 81:201–213
DOI 10.1007/s11071-015-1982-8

ORIGINAL PAPER

Experimental investigation of a rotating parametric pendulum

Panagiotis Alevras · Iain Brown · Daniil Yurchenko

Received: 23 June 2014 / Accepted: 15 February 2015 / Published online: 1 March 2015

Abstract The parametrically excited pendulum has been attracting significant interest with recently being involved in the development of a wave energy converter. The capability of establishing rotational motion is however restricted by the quite low frequency of ocean waves. Introducing a design of a tri-pendulum instead of a simple pendulum could provide a solution to that obstacle. In this paper, an experimental investigation of the response of a tri-pendulum to parametric excitation is presented. The target is to achieve rotational response of the tri-pendulum and highlight some of the particularly useful characteristics of this design such as the configurability and flexibility of its size without affecting its functionality. Experimental demonstrations of previous observations regarding the rotational response under not vertical, but tilted rectilinear, excitation are sought as well.

Keywords Parametric · Physical pendulum · Wave energy · Experimental · Planar excitation

1 Introduction

Parametric excitation is a phenomenon widely met in mechanical and electrical dynamical systems. The fundamental feature of these systems is the induction of the excitation through one of their parameters and not externally, usually through the stiffness coefficients and in some cases through the damping parameters. The center of interest of the analysis lies on the stability of the response and the demonstration of the parametric resonances. The most common example is a pendulum with periodically excited pivot. A special case yet extensively studied is the stability of the bottom equilibrium point. The linear differential equation dictating the dynamics of this case has been shown to give rise to unstable response when resonating, also classified as Mathieu equation [10].

Regarding the full dynamics of the parametric pendulum a rich variety of different types and bifurcations of the responses could be found. Among these, the stabilization of the upper equilibrium point, i.e., the stability of the inverted pendulum [13,16], as well as period doubling of the oscillating response and even chaos is observed attracting a vast number of researchers and studies [2]. Yet, the scope of this paper is concentrated on the rotational response of the pendulum. Several studies have dealt with analyzing the nature of this response, its characteristics and the relation of the excitation parameters to the appearance, and strength of the rotational attractor by analytical and numerical means [7,15].

Recently, the rotational motion of the pendulum has been viewed under the potential of developing a wave energy converter (WEC) [1,15,18]. The principle of

P. Alevras (✉) · I. Brown · D. Yurchenko
Institute of Mechanical, Process and Energy Engineering, Heriot-Watt University, Edinburgh EH14 4AS, UK
e-mail: pa132@hw.ac.uk

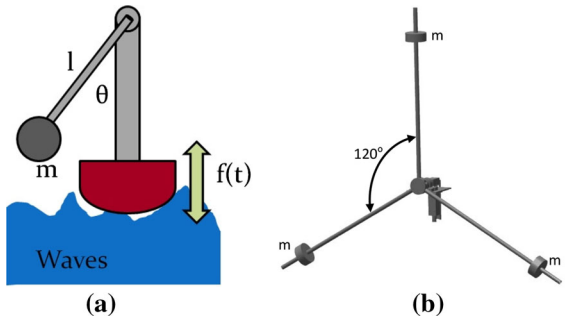

Fig. 1 **a** Sketch of the pendulum-based WEC; **b** the tri-pendulum to replace the simple pendulum

this concept (see Fig. 1a) aspires to exploit the ocean surface waves to excite the pivot of a pendulum, targeting for the latter to establish rotational motion. The main parametric resonance zone within which rotations could be more easily observed, initiates at the double frequency ratio, i.e., $\omega/\Omega = 2$ with ω the excitation frequency and Ω the pendulum's natural frequency [10]. By the time that robust rotational motion becomes achievable, attaching an electrical generator to the pivot's shaft results in direct conversion of the ocean waves' heave to electrical power. Wave energy has been recognized as one of the most promising resources of renewable energy (RE), due to the notably high power density of $8.42\,\mathrm{kW/m^2}$ compared with wind and solar energy of 0.58 and $0.17\,\mathrm{kW/m^2}$ respectively [9]. Alas, the practical and commercial exploitation of wave energy is still at an early stage with challenges in the purely technological aspect, reliability of the energy production, connection to the electricity grid and estimation of the environmental and economical impact.

The pendulum-based WEC concept provides a design which addresses a broad range of the contemporary challenges. Classified as a point absorber, a small area of the ocean surface is required for this device compared to others such as Pelamis, allowing for a greater flexibility of the array layout, reducing the influence onto the local ecosystems and local offshore economic activities. Deployment and maintenance issues are minimized due to the small size and the structural simplicity.

Since the parametric pendulum is such a fruitful dynamical system, several experimental studies have been conducted to demonstrate the properties and features of its response [5,6,12,14]. With respect to wave energy harvesting, Xu et al. [14] have studied the response of a simple pendulum to the periodic excitation provided by an electromechanical shaker. The 4-DOF mechanical model describing the dynamics of this complex system were investigated and compared against experimental results. Previous numerical studies attempting to map down the criteria of the excitation parameters so that to lead to rotational response of the pendulum were evaluated. The study tracked down and reported rotational response of the experimental rig which was also aligned to the theoretical and numerical predictions. Further on, another step was taken toward more realistic excitation supporting the proof-of-concept for this device. Lenci et al. [6] and Lenci [5] launched and reported a series of experiments where a simple pendulum attached onto a buoy was let to float on water waves generated in a laboratory wave flume. An unambiguously vast number of excitation parameter pairs were tested and different types of motion were recorded, namely oscillatory, rotary and period-doubled rotations.

However, there is a devastating drawback related to the technological feasibility of such a project stemming from the nature of the resource. Understanding the ocean waves behavior is not a new topic in engineering and extends further from energy harvesting. It has been concluded that ocean waves traveling isolated from their generation area (swells) propagate in seas resulting in oscillatory motion of the surface with an average period of 8–10 s [3]. Considering the requirement for the frequency ratio in order to enter the primary resonance zone where the region of the excitation parameters leading to rotations is much wider, one would have to design a simple pendulum approaching 100 m in length. Clearly, such an option is out of question from many standpoints. It is indicative of this limitation that the previous experimental studies concerned with wave energy harvesting, had to resort to either much larger excitation frequencies [14] or redirect to the secondary resonance zone ($\omega/\Omega = 1$).

In this paper, an experimental investigation of the concept is conducted targeting to approach conditions closer to the realistic data observed in sea. Attempting to overcome the resource-related limitations, the simple pendulum design is withdrawn and replaced by a special design of a physical pendulum, the tri-pendulum, consisting of three simple pendulums equally spaced at 120° and attached to a hinge, thus sharing a common pivot (Fig. 1b). This design has been introduced

and analyzed previously [17] with respect to its configurable natural frequency and inertia. Moreover, a numerical study setting the ground for the herein presented experiments was conducted. Here, a sinus-like excitation is imposed onto the tri-pendulum pivot with higher amplitude and lower frequency than before. In that sense, the scope of this paper is to produce and report experimental proof in two directions. First, showing the configurable property of the tri-pendulum with respect to establishing rotations and second, put the revisited WEC concept up to the task of demonstrating rotational motion under more realistic conditions as long as wave energy harvesting is concerned.

2 Experimental setup

In this section, the experimental rig that has been used to demonstrate aspects of the functionality of a tri-pendulum design for the discussed WEC is presented in detail. Previously, the dynamics of the idealized system have been investigated with respect to the natural frequency that could be achieved, which is crucial in order to fall within the primary parametric resonance zone. The idealized system is meant as a tri-pendulum with three lumped masses and massless arms, shaft etc. The inertia of the system has been also jointly addressed, since the power generation is directly related to the inertia. Here, a brief overview of the equations of motion and the proposed idea is performed as well as a detailed technical description of the experimental rig in parts and as a whole.

2.1 The model

The underlying idea consists of a system capable of achieving the natural frequency that is required for the primary parametric resonance given the limitations of the natural resource in the ocean. It is proposed to adopt a design consisting of three arms equally spaced at 120°, as it is illustrated in the drawing in Fig. 1b. The basic design refers to three equal masses distributed at the three arms. The frequency variations are realized by placing these masses at different distances and specifically, two of them at L_2 and the third one at $L_1 > L_2$. Of course, a much greater flexibility underlies by varying the masses that each arm carries as well as introducing three unequal distances. However, this paper is only concerned with the basic design, both in the presentation of the model and the experimental investigation. In the case of the basic design then, with the pivot vertically excited by $f(t)$, the equation of motion reads:

$$(I_c + I_v)\,\ddot{\theta} + c\dot{\theta} + m(L_1 - L_2)\left[g + \ddot{f}(t)\right]\sin\theta = 0 \tag{1}$$

with I_c being the constant inertia of the parts free to move in the angular space and I_v the adjustable inertia. Also, c is the viscous damping coefficient modeling the energy losses, m the mass held by each arm and θ the angular displacement.

It is evident that the natural frequency of Eq. (1) is mostly affected from the varying lengths L_1 and L_2 and indeed, by their difference. Thus, the achievable values of the natural frequency are decoupled by the length, contrary to the case of a simple pendulum [17]. One should note, however, that the range of admitted values is not infinite, but it is constrained by both I_c and I_v. Thus, given an excitation frequency ω, one could properly configure the tri-pendulum through L_1 and L_2 so that the parametric system would fall into the range of the primary resonance, and specifically in the corresponding rotational region. For the shake of an example, if the given $\omega = 1$ rad/s, then a simple pendulum would need to extend to 39.24 m in order to establish $\omega/\Omega = 2$, while one possible configuration of the idealized tri-pendulum is $L_1 = 0.52$ m and $L_2 = 0.5$ m.

Having raised then the potential usage of a tri-pendulum, the development of an experimental rig could be discussed. The main requirements could be condensed to the following: (a) vertical periodic motion of the tri-pendulum (Fig. 1b) (b) amplitude and frequency of that considerably close to the realistic observations (c) capability of varying the frequency at will (d) recording of the angular response. The realization of this design would also need to comply with constrains on the total size imposed by the indoor infrastructure. A computer-based drawing of the experimental rig is shown in Fig. 2. First of all, the source of the vertical motion has to be chosen. A crank-arm attached to a motor placed on the bottom of the rig will function as a reciprocal piston-like mechanism as to provide the vertical excitation to the tri-pendulum. A frame is required to support the tri-pendulum which is allowed though to move up and down through a roller-rail system with the latter rigidly attached to the frame. The design of the experiments targets an excitation amplitude of 0.5 m at

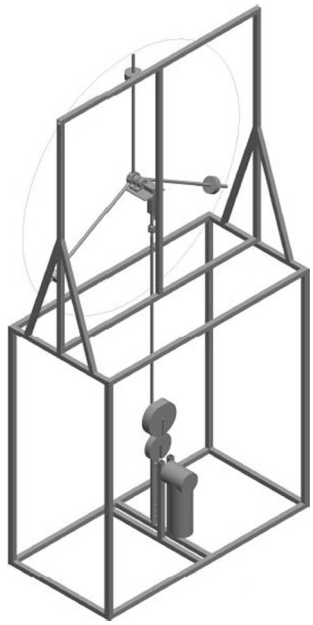

Fig. 2 Drawing of the full experimental rig

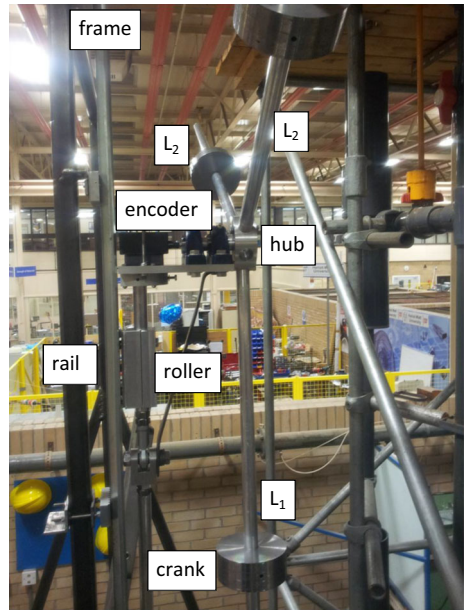

Fig. 3 The apparatus subsystem of the tri-pendulum

most. Furthermore, the radius of the tri-pendulum at test is designed at 1 m. The circular motion of the crank-arm of the motor is transduced to rectilinear through a crank connecting the edge of the crank-arm to the pivot of the tri-pendulum. In order to render the superharmonics of the resulting motion negligible, the length of this crank has to be considerably bigger than the amplitude. Considering all these constrains, the design of the frame is led to a total 4 m in height, 2 m in width and 1 m in depth.

2.2 Technical description

The experimental apparatus could be divided into three major subsystems; the tri-pendulum, the mechanism that provides the motion and ensures its structural integrity and the data acquisition subsystem extending from the angular sensor to the post-processing of the data. In this part of the paper, a description of the experimental rig will be provided and the preliminary tests of the damping identification in the tri-pendulum system will be discussed.

2.2.1 Tri-pendulum part

The core of this experimental study lies within the tri-pendulum part (Fig. 3). In this figure, one could see at the bottom, the crank that transfers the circular motion provided by the motor to the tri-pendulum subsystem. The plate holding the bearings that carry the shaft of the tri-pendulum is attached to the frame through a roller that is allowed to perform translational motion within a rail. The latter is rigidly bolted onto the frame. The frequency configuration is achieved through the position of the masses that the tri-pendulum carries. At the end of the shaft is an adapter and coupling to connect an angular encoder to record the angular response of the tri-pendulum. The coupling was added between the shaft adapter and the encoder to allow for small misalignments and vibrations.

The two plummer bearings and encoder are mounted on an aluminum plate. Under this plate, there is an adapter to connect the vertical rod, or the "piston" of the reciprocal mechanism, to the tri-pendulum. The bottom edge of this rod is threaded for a spherical joint to be mounted, intended to connect the crank to the tri-pendulum subsystem. This is necessary since the reciprocal mechanism forces the crank to move in the vertical plane, while the roller has to pushed upwards and drawn downwards on a straight line.

2.2.2 Motorizing

The experimental apparatus is housed in a frame split in two parts. The top section is a 2D 2×2 m frame in

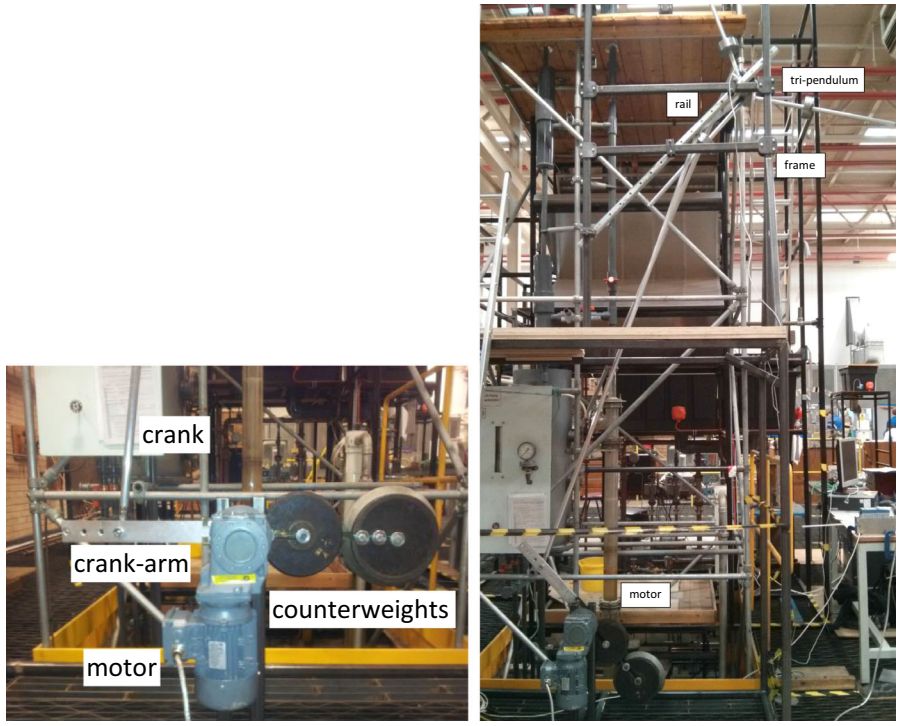

Fig. 4 Parts of the apparatus; **a** The motorizing subsystem of the tri-pendulum; **b** view of the full experimental rig. The rail is tilted from the vertical direction resulting in excitation at a constant angle

the middle of which a vertical bar allows the mounting of the 1.5 m T-rail along its length. The bottom section of the frame is a box measuring $2 \times 2 \times 1$ m with two additional bars traversing the bottom of the frame to locate the verticals bars on which the motor and gearbox drive is mounted (Fig. 4a).

The top edge of the crank is connected through a spherical joint to the vertical rod where the roller is clamped on. The length of the crank had to be considerably larger than the amplitude of the excitation. This is imposed so that the superharmonics that arise in the motion of the working point of the reciprocal mechanism (the top egde of the crank) would be rendered negligible thus approximating a sinusoidal motion. Since the designed maximum amplitude is 0.5 m, a length of 2.4 m for the crank is chosen to overcome the discussed issue. Note that this leads to a required height for the frame of >3.5 m with the total design of 4m-high frame covering that.

The bottom edge of the 2.4-m-long crank is then connected through another spherical joint to the crank-arm. The crank is attached to the crank-arm through a studded rod end and can be placed at any of the four drilled threaded holes on the crank-arm. These holes basically provide four positions for the connection at 0.35, 0.4, 0.45, 0.5 m, forming four different radii of the reciprocal mechanism. In that way, each of these positions regulates the amplitude of the excitation. However, the crank-arm extends in both ways with respect to the shaft of the motor (Fig. 4a). One side is used for the connection with the crank and the transfer of the motion to the tri-pendulum. The other one carries counterweights in order to reduce the load applied to the motor gearbox and soften impulse loads arising at 0 and π angle of the crank-arm position.

The reciprocal mechanism to simulate waves is driven by an electric motor coupled with a gearbox of 22.78:1 ratio. The speed of the motor controlling the frequency of the parametric excitation was set through an inverter.

2.2.3 Measurement

For measuring the angular displacement of the excited tri-pendulum, an angular encoder with resolution of 3000 counts per revolution, outputting a digital signal was attached to the tri-pendulum shaft (see Fig. 3). The signal from the encoder was sent to a DAQ card,

which was then connected to a computer running Labview software. Any post-acquisition data processing required on the raw data was done in MATLAB before plotting for analysis.

3 Results and analysis

In this section, the results of the experimental efforts concerned with the described tri-pendulum and rig are presented. The main goal driving the actualization of these experiments is twofold. On a first level, it is sought to demonstrate the equivalence of a realistic tri-pendulum design to a simple pendulum of unrealistic size. This equivalence is dictated by the need to fall within the rotational parameter regions in the context of developing a pendulum-based WEC. On a second level, the multiplicity of the possible configurations standing as kinematically identical solutions is raised. This is rather important considering the direct relation of not only the magnitude of mass m to the total inertia of the system, but of the distances L_1 and L_2 as well, and the consequential implications onto the potential generated power.

3.1 Preliminaries

Before getting into the main body of the experiments, one would have to clarify specific issues concerning the calculation of the natural frequency in the realized system, the damping accompanying the angular response of the pendulum, the modeling of the experimentally observed responses, as well as the post-processing of the data involved in the presentation of the results.

3.1.1 Natural frequency Ω

A short note on the calculation of the natural frequency of the experimental tri-pendulum is required since the idealized system can no longer describe it. This value is thought of as the natural frequency of an equivalent simple lumped mass pendulum and so, considering Eq. (1) it is defined as:

$$\Omega_{eq} = \sqrt{mg\,(L_1 - L_2)\,/\,(I_c + I_v)} \tag{2}$$

I_c refers to the inertia of the necessary parts for the structural realization of the tri-pendulum and include the moment of inertia with respect to the pivot O, of the shaft, the disk (or hub), the spokes and the masses. Since these are solid bodies, their moment of inertia, following Stainer's theorem, needs to consider the inertia around an axis perpendicular to the plane of angular motion. The varying part, I_v, refers to the moment of inertia of the center of mass of the masses carried by the spokes with respect to the pivot O, directly related to and affected by the lengths L_1 and L_2 and thus characterized as varying.

This design aspires to overcome the limitations on the practical application of the discussed WEC and to provide flexibility and configurability. In [17], an extended presentation of the resulting Ω_{eq} has been included in conjunction with the development of the moment of inertia. This part of the analysis is intentionally omitted and the reader is referred to that paper for this issue.

3.1.2 Damping identification

The selection of the excitation parameters and the possible combinations of the lengths L_1 and L_2 depend on the energy damped per cycle. This is expressed through the well-known effect of increasing viscous damping coefficient onto the parameter space response. Higher damping requires higher input energy meaning that the map of the different types of responses (oscillatory, rotary, etc.) is pushed to higher excitation amplitudes. Thus, in order to design a series of experiments that could be predicted by numerical simulations, the latter should be conducted for a viscous damping coefficient that closely models the damped energy. Before proceeding to the main part of the experiments, a series of free vibrations tests were undertaken to evaluate the energy losses. The logarithmic decrement method was applied and an average value of $c = 0.10$ kg m/s has been found which will be used for the numerical simulations. Of course, the viscous damping coefficient β will depend on the adjustable inertia as well since $2\beta = c/(I_c + I_v)$, but due to the very small value of the damping, these changes will not drastically influence the numerical construction of the map of the responses (Fig. 5a, b).

The construction of a map with respect to the excitation parameters separating the different types of responses has been discussed previously [17] and will be used as a guide for the targeted experimental tests which in turn will be used to verify the capabil-

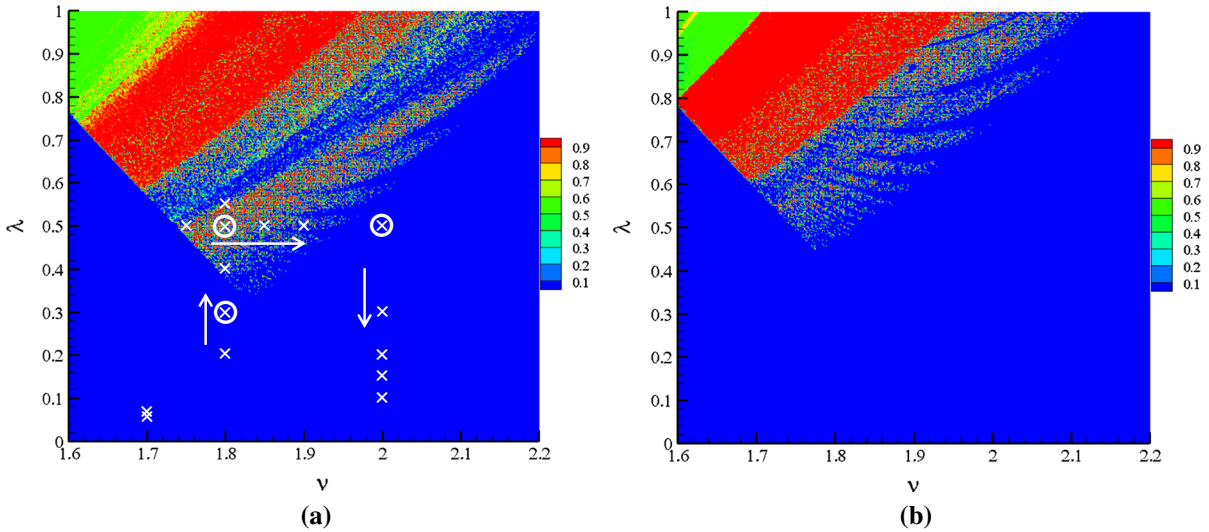

Fig. 5 Numerically constructed PSM of the response of the tri-pendulum to vertical periodic excitation for $\theta(0) = 0.01\pi$ rad and $\dot{\theta}(0) = 0.0$rad/s. *Colormap* characterizes the percentage of rotational motion in the steady-state response with blue $< 10\,\%$ and red $> 90\,\%$. The *points* marked with $\times$ denote the different parameter pairs that were recorded irregardless of the multiplicity of the tri-pendulum configuration. The *points* marked with $\circ$ denote those points that were used to record identical response with different L_1, L_2 configuration. **a** Non-dimensional damping coefficient $\gamma = 0.01$; **b** $\gamma = 0.05$

ity of rotations for different configurations of the tri-pendulum, i.e., of L_1 and L_2.

3.1.3 Parameter space maps (PSM)

Modeling the response of the tri-pendulum follows a rationale that places rotational motion under the microscope. The target is to characterize the rotational capability for a range of the influencing parameters which are expressed through $\nu = \omega/\Omega$ and $\lambda = A\omega^2/g$ where A is the excitation amplitude. This selection is not random but emerges by a common useful transformation of the time variable in Eq. (1) [1,18].

Further on, an effort to predict through standard numerical modeling the response of the tri-pendulum would have to specify the definition of the excitation $f(t)$. In the studies of the parametric pendulum, a pure periodic sinusoidal function is commonly exciting the system. This experimental study utilizes a reciprocal mechanism to approach this. However, the motion of the working point (i.e., the pivot) is known to include superharmonics and the acceleration could be specifically found as:

$$\ddot{f}(t) = \omega^2 r \left(\cos\omega t + \frac{\cos 2\omega t}{j}\right) \tag{3}$$

where r is the crank-arm radius or else the amplitude of the excitation and j the ratio of the length of the crank over r. In [17], the influence of j onto the shape of the PSM has been investigated. It was found that $j > 4$ renders the effect of the superharmonics negligible as long as the topology of rotations in the parameter space is concerned. In the experimental setup, $max(j) = 4.8$ and thus, modeling the response to a monochromatic excitation is sufficient.

Figure 5a shows the PSM for a low non-dimensional damping coefficient, $\gamma = c/(I\Omega) = 0.01$ and for $\theta(0) = 0.01\pi$ rad and $\dot{\theta}(0) = 0.0$ rad/s. Red indicated the desired region of > 90 % rotations with blue denoting the < 10 %. This map is constructed by counting the rotational motion for each case in the steady-state response. A detailed description on the production of PSMs could be found in [1,18]. Of course, once I and Ω change, γ changes with the possibility of an oscillatory point to become rotary with increased $I\Omega$ because the PSM itself would have been drawn downwards. Yet, this change would have to be enormous since c is of very small value and this issue does not affect the herein experiments.

It is worth noting that the conducted experiments were attempted to match the initial conditions that were used in the PSMs. However, it is extremely difficult to

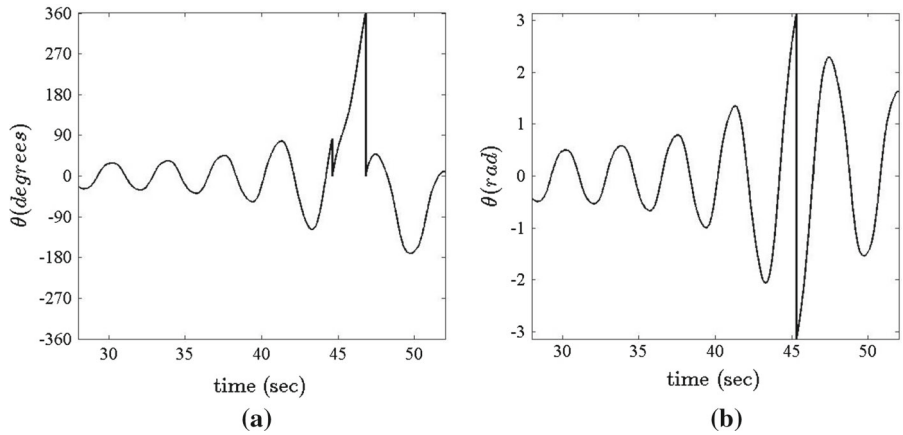

Fig. 6 Angular output of the encoder; **a** data as were recorded through the DAQ subsystem. Measurement is done in *degrees*, covering a range of 720° and reporting inexistent jumps; **b** data resulting from post-processing of the raw data in Fig. 6**a** within the MATLAB environment. The issues raised have been corrected

assure precision and on the other hand, several uncertainties in the parts of the rig and their assembly would cancel such efforts. Yet, the best possible care was taken to initiate every test as close as possible to the given initial conditions. A study aiming to extend the current results to incorporate considerations of the attractors' robustness could largely benefit from the construction of basins of attraction and the assessment of their robustness through the dynamical integrity concept and the integrity factor [8].

One aspect of the goal of the herein presented experiments is to demonstrate agreement between the numerical prediction of the response through PSMs with the experimentally recorded response of the tri-pendulum. To that end, the marked points in the PSM in Fig. 5a are targeted and investigated by use of the experimental rig. These points are selected in such a way so that experimental verification of the prediction of their response would attribute consistency to the PSM.

On a second level, the flexibility and configurable capability of the design is sought to be demonstrated by attempting to achieve identical response attached to one point in the PSM, with different values of L_1 and L_2.

3.1.4 Post-processing

The angular sensor is an optical encoder that is attached to the tri-pendulum's shaft and has three digital outputs. Two of these are used to count how many of the 3000 marks dividing the circle have been observed. In that way, the sensor gives exact information on the total angle run from the initiation of the measurements. The third one, known also as the index signal I, is used to signify the crossing of a unique mark which is utilized to denote a full revolution.

However, when the sensor powers up, it assumes an angular value equal to zero and this is because it cannot perform explicit angle measurements but only changes in angular position. Then, at the first activation of the index signal I, the output is normalized to zero again which results in a falsified output as could be seen in Fig. 6a. It could also be seen that the range of the measurements extends up to two revolutions. In order to correct these two issues, a MATLAB script has been applied normalizing the output within $[-\pi, \pi]$ and correcting the false jump. Note that the post-processed data assume for zero degrees the correct equilibrium point as this was the starting point of each measurement. This normalization leads to jump from $-\pi$ to π when the motion is rotational, which nevertheless causes no difficulties except for the calculation of the velocity where they are accounted for in the post-processing script.

As a final note before the presentation of the experimental results, the initial conditions of the tests have to be addressed. Recording of the angle would have to start as early as to capture the tri-pendulum at equilibrium, thus ensuring consistency of the measurements. However, due to the trivial stability of the equilibrium, the system had to be displaced even slightly by an external source in order for the excited response to unfold. The mathematical side of this could also be understood by observing Eq. (1).

3.2 Vertical excitation

The first set of experiments is related to using the PSM in Fig. 5a as a guide for predicting the response of

Table 1 Specifications of the experimentally recorded responses of the tri-pendulum to vertical excitation

ω (rad/s)	r (m)	L_1 (m)	L_2 (m)	Ω (rad/s)	I_{tot} (kg m^2)	l_{eq} (m)	ν	λ	Response
1.255	0.400	0.400	0.370	0.741	2.533	17.876	1.690	0.060	F
1.255	0.450	0.400	0.370	0.741	2.533	17.876	1.690	0.070	F
2.215	0.400	0.298	0.249	1.235	1.488	6.435	1.800	0.200	F
2.712	0.400	0.390	0.300	1.506	1.839	4.323	1.800	0.300	F
3.149	0.400	0.281	0.200	1.743	1.233	3.228	1.800	0.400	O
3.744	0.350	0.430	0.249	2.078	1.944	2.273	1.800	0.500	R
3.678	0.400	0.321	0.200	2.039	1.347	2.360	1.800	0.550	R
3.502	0.400	0.410	0.249	2.001	1.863	2.451	1.750	0.500	R
3.502	0.400	0.481	0.300	1.947	2.214	2.587	1.800	0.500	R
3.502	0.400	0.386	0.249	1.892	1.772	2.741	1.850	0.500	R
3.744	0.350	0.403	0.249	1.971	1.838	2.525	1.900	0.500	R
3.502	0.400	0.533	0.350	1.750	2.770	3.202	2.000	0.500	O
3.502	0.400	0.433	0.300	1.753	2.006	3.191	2.000	0.500	O
2.758	0.400	0.300	0.240	1.383	1.452	5.128	1.990	0.310	O
2.215	0.400	0.288	0.249	1.112	1.460	7.934	2.000	0.200	F
1.918	0.400	0.277	0.249	0.952	1.431	10.829	2.020	0.150	F
1.566	0.400	0.268	0.249	0.790	1.480	15.701	1.980	0.100	F

the tri-pendulum. Let us note again that this map can only be used as guide and not as an exact predictor since the damping coefficient is approximated as a constant value among the different trials. The specifications of the configuration of the lengths and the rest of the parameters for these experiments are concentrated in Table 1. For each case, the parameter set ν, λ is reported with the experimental response characterized as {R,O,F} for rotating, oscillating and fixed point steady-state response respectively. The target is for points leading to rotations to demonstrate agreement with the predictions.

First, two points were investigated with very low λ (0.06 and 0.07), expected to end up in a fixed point response, something that was verified. Further on, moving to a frequency ratio $\nu = 1.8$, the gradual increase in the amplitude was expected to drive the tri-pendulum to bifurcate from fixed point to rotations through oscillations. In fact, starting from $\lambda = 0.2$, for which the response could not escape the equilibrium well, the first rotating point was found for $\lambda = 0.5$ as expected. A second point for $\lambda = 0.55$ was recorded rotating so that the entrance to the rotational region would be further supported.

Next, it was attempted to cross the right boundary of the rotational region. The non-dimensional excitation amplitude was fixed at $\lambda = 0.5$ and the advance of the investigation was performed through changing ν, expecting to cross the right boundary and bifurcate from rotations to oscillations. Indeed, the far left point was for $\nu = 1.75$, predicted to have a rotational response, as in fact was experimentally recorded. The rotational motion should be sustained for frequency as high as $\nu = 1.9$, totaling up to 4 recorded points leading to rotations. As soon as ν was increased to 2, the rotational motion bifurcated to oscillatory.

Then, decreasing the amplitude λ, the PSM informed us of returning to a fixed point response as the input energy would decrease, a development that was recorded for $\lambda < 0.310$, and is reported in Table 1. One could note that different configurations of L_1 and L_2 were used with no particular constraint as with the simple pendulum.

However, the capability of achieving the same natural frequency with different layouts, and thus decoupling the non-dimensional parameter pair (ν, λ) from the size of the device is demonstrated in the second set of the experiments, shown in Table 2. This table is divided into three sets. Each of them corresponds to one point in the PSM marked with $\circ$ in Fig. 5a. The target here is to use different layouts within each set, keeping however the controlling parameters constant and thus

Table 2 Three points from the PSM corresponding to different responses (R, O, F) with three different configurations of L_1, L_2 each

ω (rad/s)	r (m)	L_1 (m)	L_2 (m)	Ω (rad/s)	I_{tot} (kg m^2)	l_{eq} (m)	ν	λ	Response
3.502	0.400	0.284	0.200	1.946	1.029	2.591	1.800	0.500	R
3.502	0.400	0.481	0.300	1.947	2.214	2.587	1.798	0.500	R
3.502	0.400	0.610	0.350	1.945	3.186	2.593	1.800	0.500	R–O[a]
2.712	0.400	0.246	0.200	1.512	0.933	4.293	1.794	0.300	F
2.712	0.400	0.390	0.300	1.506	1.839	4.323	1.801	0.300	F
2.712	0.400	0.471	0.350	1.505	2.476	4.329	1.802	0.300	F
3.502	0.400	0.265	0.200	1.754	0.979	3.187	1.996	0.500	O
3.502	0.400	0.433	0.300	1.753	2.006	3.191	1.997	0.500	O
3.502	0.400	0.533	0.350	1.750	2.770	3.202	2.001	0.500	O

[a] Extreme vibrations caused by the large inetria did not allow rotational motion to settle

recording the same response. The results reported in Table 2 validate the configurable attribute of the tri-pendulum with the exception of one point were the inertia value was too big to be properly supported by the experimental rig. For the sake of an example, two different layouts of $L_1 = 0.284\,\text{m}$-$L_2 = 0.2\,\text{m}$ and $L_1 = 0.481\,\text{m}$-$L_2 = 0.3\,\text{m}$ lead to the same point in the PSM and fall into the rotational attractor. This flexibility in selecting the lengths is very important from the energy harvesting standpoint, since the bigger the moment of inertia the bigger the generator that could be attached to the rotor's shaft. Moreover, the overall size of the device compared to a simple pendulum has been reduced several times for all the examined cases. This is evident by simply comparing the length of a simple pendulum, l_{eq}, that would be required to achieve the same parameter pair with the longest of the spokes, L_1, for each of the cases reported in the tables.

In Fig. 7, the recorded post-processed signals coming from two different sets, one rotational and one oscillatory are shown for consistency. The angular signal includes the transient period as well, while the velocity and the phase space incorporate only the steady-state response.

3.3 Tilted excitation

Previous studies [4,11] have reported that planar excitation of the pendulum's pivot draws the threshold for rotations toward lower λ values. Here, this numerically supported argument is investigated experimentally.

Planar excitation is thought to be the forcing of the pivot outside the vertical line. The elliptical trajectory of the pivot and the rectilinear one but at a tilt angle from the vertical direction have been studied by means of analytical [11] and numerical [4] methods. Due to the limitations of the rig, the only possible alteration in the imposition of the excitation was to divert its direction. Therefore, instead of a vertical driving of the tri-pendulum, the rail that guides its motion is tilted at 10° with respect to the vertical axis, as could be seen in Fig. 4b. Hence, the tri-pendulum is excited by a planar force and expected to demonstrate rotations for lower λ values.

In order to test this premise, direct comparison with the experimental results obtained from the vertical driving is sought. In particular, the points in the PSM in Fig. 5(a) consisting an upwards path, denoted by the up-pointing arrow, are revisited. Starting from a point which already demonstrated rotational response $\nu = 1.800$, $\lambda = 0.500$, the amplitude is decreased down to the other points that were tested ($\lambda = 0.4$ and 0.3). This corresponds to the first three cases presented in Table 3. Comparing the response to the vertical excitation with the one to the tilted one, it could be extracted that the rotational region expands to lower λ values. Instead of the oscillatory response observed for $\lambda = 0.4$ and the fixed point one ($\lambda = 0.3$), purely rotational response was recorded (see Fig. 8a).

Moreover, another characteristic of the system under tilted excitation is that the fixed point response observed for vertical excitation transforms to oscillatory [4]. Decreasing λ does not lead to equilibrium but rather in an steady-state oscillatory response with its amplitude reducing with lower λ. Indicatively, one could see the last three cases presented in Table 3 and the recorded signal in Fig. 8b.

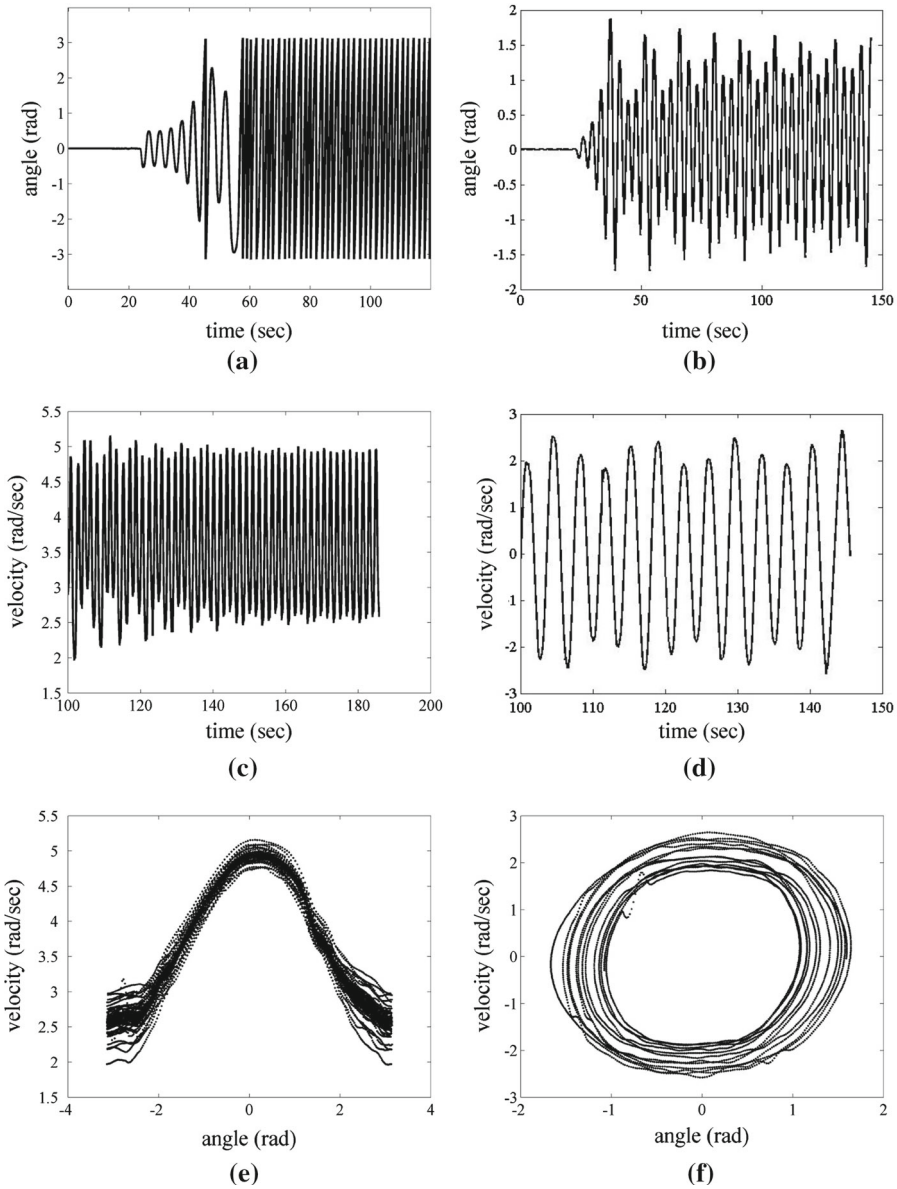

Fig. 7 Experimental post-processed recorded response to vertical excitation; rotating response for $\nu = 1.800,\ \lambda = 0.500$ (a–c–e); oscillating response for $\nu = 2.000,\ \lambda = 0.500$ (b–d–f)

Table 3 Specifications of the experiments and responses with the excitation in a tilted line

ω (rad/s)	r (m)	L_1 (m)	L_2 (m)	Ω (rad/s)	I_{tot} (kg m^2)	l_{eq} (m)	ν	λ	Response
2.900	0.350	0.325	0.249	1.613	1.355	3.771	1.800	0.300	R
3.348	0.350	0.358	0.249	1.859	0.671	2.839	1.800	0.400	R
3.744	0.350	0.399	0.249	2.080	1.608	2.268	1.800	0.500	R
3.744	0.350	0.182	0.130	2.024	0.585	2.395	1.850	0.500	R
3.348	0.350	0.176	0.140	1.674	0.602	3.500	2.000	0.400	O
2.900	0.350	0.298	0.250	1.319	1.280	5.641	2.200	0.300	O
2.368	0.350	0.276	0.250	0.986	1.219	10.083	2.400	0.200	O

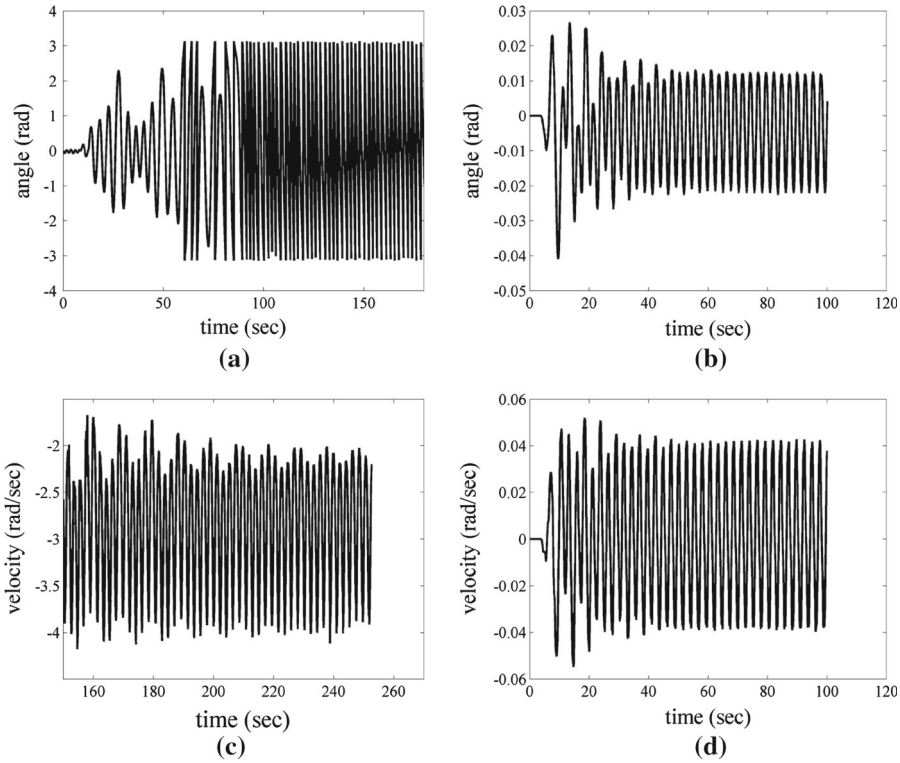

Fig. 8 Experimental post-processed recorded response to tilted excitation; rotating response for $\nu = 1.800,\ \lambda = 0.300$ (a–c); oscillating response for $\nu = 2.400,\ \lambda = 0.200$ (b–d)

4 Conclusions

In this paper, an experimental investigation of the response of a parametrically excited physical pendulum is presented. The system at hand, a tri-pendulum, consists of three simple pendulums integrated into one. The interest is focused onto the capability of establishing rotational response in view of a concept for wave energy harnessing. The purpose of introducing this design is to overcome the limitations imposed by the physical resource of ocean waves onto the capability of a simple pendulum to fall into the primary parametric resonance.

The initiative for the herein presented experiments is twofold. First, a correspondence to the response exhibited by a simple pendulum was sought. In that sense, the target of the first set of the experiments was to demonstrate the equivalence between the response of the tri-pendulum to the one of a simple pendulum under the same exciting conditions. The benefit attached to the tri-pendulum however, is that of its size. Whereas a simple pendulum would require an extremely long structure, sometimes even unfeasible for technological applications, the tri-pendulum would provide an equivalent behavior (i.e., rotational) with not only realistic size but a multiplicity of configurations. Hence, this first sets of the experiments demonstrated that one could use the numerically constructed PSM characterizing the type of the response for the tri-pendulum with a direct equivalence.

Moreover, a second set of experiments was conducted, concerned with just three exciting cases, unique in the non-dimensional parameter space that controls the nature of the response. For each of these points, different configurations of the distances of the masses from the pivot were tested, resulting though in the same parameter space point, only by changing the distances and keeping the rest of the parameters constant. This is impossible to be accomplished by a simple pendulum which natural frequency is one-on-one related to its length. Thus, the experiments demonstrated the capability of the tri-pendulum to change its size but not the controlling parameters that regulate its response. This is a rather important characteristic when energy harnessing is concerned, holding a relatively strong decoupling of the size of the device with its functionality. One needs only to consider the potential of an enlarged generator attached to the device's rotor with-

out the functionality being affected since the lengths L_1 and L_2 could be configured to maintain the exact same functionality.

Last but not least, a modification of the classical vertical excitation was examined in the available experimental rig. The direction of the driving force was tilted by 10° and the conclusions of previous numerical studies were partly tested. Particularly, it had been found that a tilted direction of the excitation would draw the λ threshold for rotations downwards. Indeed, it has been experimentally found that points in the PSM that would fall into the oscillatory or fixed point attractor, would inherit rotational response only by shifting the direction of the excitation.

Acknowledgments This study would not have been realized without the dedication and professionalism of the technicians in the mechanical workshop in Heriot-Watt University. The authors would particularly like to express their gratitude to Mr. Richard Kinsella and Mr. Ian Harrower.

References

1. Alevras, P., Yurchenko, D.: Stochastic rotational response of a parametric pendulum coupled with an SDOF system. Probab. Eng. Mech. **37**, 124–131 (2014)
2. Chen, X., Jing, Z., Fu, X.: Chaos control in a pendulum system with excitations and phase shift. Nonlinear Dyn. **78**, 1–11 (2014)
3. Cruz, J.: Ocean Wave Energy. Current Status and Future Perspectives. Springer, Berlin (2008)
4. Horton, B., Sieber, J., Thompson, J.M.T., Wiercigroch, M.: Dynamics of the nearly parametric pendulum. Int. J. Nonlinear Mech. **46**, 436–442 (2011)
5. Lenci, S.: On the production of energy from sea waves by a rotating pendulum: a preliminary experimental study. J. Appl. Nonlinear Dyn. **3**(2), 187–201 (2014)
6. Lenci, S., Brocchini, M., Lorenzoni, C.: Experimental rotations of a pendulum on water waves. J. Comput. Nonlinear Dyn. **7**(1), 011,007 (2012)
7. Lenci, S., Pavlovskaia, E., Rega, G., Wiercigroch, M.: Rotating solutions and stability of parametric pendulum by perturbation method. J. Sound Vib. **310**, 243–259 (2008)
8. Lenci, S., Rega, G.: Experimental versus theoretical robustness of rotating solutions in a parametrically excited pendulum: a dynamical integrity perspective. Phys. D: Nonlinear Phenom. **240**(9–10), 814–824 (2011)
9. McCormick, M.E.: Ocean Wave Energy Conversion. Courier Dover Publications, Mineola, NY (2013)
10. Nayfeh, A.H., Mook, D.T.: Nonlinear Oscillations. Wiley, New York (1979)
11. Pavlovskaia, E., Horton, B., Wiercigroch, M., Lenci, S., Rega, G.: Approximate rotational solutions of pendulum under combined vertical and horizontal excitation. Int. J. Bifurc. Chaos **22**(5), 1250,100 (2011)
12. Sartorelli, C., Lacarbonara, W.: Parametric resonances in a base-excited double pendulum. Nonlinear Dyn. **69**, 1679–1692 (2012)
13. Semenov, M., Shevlyakova, D., Meleshenko, P.: Inverted pendulum under hysteretic control: stability zones and periodic solutions. Nonlinear Dyn. **75**(1–2), 247–256 (2014)
14. Xu, X., Pavlovskaia, E., Wiercigroch, M., Romeo, F., Lenci, S.: Dynamic interactions between parametric pendulum and electro-dynamical shaker. ZAMM **87**, 172–186 (2007)
15. Xu, X., Wiercigroch, M., Cartmell, M.P.: Rotating orbits of a parametrically-excited pendulum. Chaos Soliton Fractal **23**, 1537–1548 (2005)
16. Yabuno, H., Miura, M., Aoshima, N.: Bifurcation in an inverted pendulum with tilted high-frequency excitation: analytical and experimental investigations on the symmetry-breaking of the bifurcation. J. Sound Vib. **273**, 493–513 (2004)
17. Yurchenko, D., Alevras, P.: Dynamics of the N-pendulum and its application to a wave energy converter concept. Int. J. Dyn. Control **1**(4), 290–299 (2013)
18. Yurchenko, D., Naess, A., Alevras, P.: Pendulum's rotational motion governed by a stochastic Mathieu equation. Probab. Eng. Mech. **31**, 12–18 (2013)